Author Manuscript

Author Manuscript

Author Manuscript

Author Manuscript

HHS Public Access

Author manuscript

ACS Chem Biol. Author manuscript; available in PMC 2018 December 15.

Published in final edited form as:

ACS Chem Biol. 2017 December 15; 12(12): 3093–3102. doi:10.1021/acschembio.7b00688.

Co-culture of Marine Invertebrate-Associated Bacteria and Interdisciplinary Technologies Enable Biosynthesis and Discovery of a New Antibiotic, Keyicin

Navid Adnani[1], **Marc Chevrette**[2,3], **Srikar N. Adibhatla**[1], **Fan Zhang**[1], **Qing Yu**[1], **Doug R. Braun**[1], **Justin Nelson**[4], **Scott W. Simpkins**[4], **Bradon R. McDonald**[2], **Chad L. Myers**[4,5], **Jeff S. Piotrowski**[6], **Christopher J. Thompson**[7], **Cameron R. Currie**[2], **Lingjun Li**[1], **Scott R. Rajski**[1], and **Tim S. Bugni**[1,*]

[1]Pharmaceutical Sciences Division, School of Pharmacy, University of Wisconsin, Madison, Wisconsin 53705, United States

[2]Department of Bacteriology, University of Wisconsin, Madison, Wisconsin 53705, United States

[3]Department of Genetics, University of Wisconsin, Madison, Wisconsin 53705, United States

[4]Bioinformatics and Computational Biology Program, University of Minnesota-Twin Cities, Minneapolis, Minnesota 55455, United States

[5]Department of Computer Science and Engineering, University of Minnesota-Twin Cities, Minneapolis, Minnesota 55455, United States

[6]Yumanity Therapeutics, Cambridge, Massachusetts 02139, United States

[7]Bruker Daltonics, Billerica, Massachusetts 01821, United States

Abstract

Advances in genomics and metabolomics have made clear in recent years that microbial biosynthetic capacities on Earth far exceed previous expectations. This is attributable, in part, to the realization that most microbial natural product (NP) producers harbor biosynthetic machineries not readily amenable to classical laboratory fermentation conditions. Such “cryptic” or dormant biosynthetic gene clusters (BGCs) encode for a vast assortment of potentially new antibiotics and, as such, have become extremely attractive targets for activation under controlled laboratory conditions. We report here that co-culturing of a *Rhodococcus* sp. and a *Micromonospora* sp. affords keyicin, a new and otherwise unattainable bis-nitroglycosylated anthracycline whose

[*]**Corresponding Author:** Tim S. Bugni, Pharmaceutical Sciences Division, School of Pharmacy, University of Wisconsin-Madison, Madison, WI 53705, United States. Email: tbugni@pharmacy.wisc.edu.

Supporting Information

All experimental procedures with complete spectroscopic data sets and spectra, S1–S7 spectroscopic characterizations/logic along with validating modeling and DFT calculations, all chemical genomics data (some as excel files) and noted BGC information for keyicin and nogalamycin as well as chemical structures for the noted anthracyclines are provided as supporting information. This material is available free of charge via the Internet at http://pubs.acs.org.

ORCID

Tim S. Bugni: 0000-0002-4502-3084

Notes

The authors declare no competing financial interest.

Author Manuscript Author Manuscript Author Manuscript Author Manuscript

mechanism of action (MOA) appears to deviate from those of other anthracyclines. The structure of keyicin was elucidated using high resolution MS and NMR technologies, as well as detailed molecular modeling studies. Sequencing of the keyicin BGC (within the *Micromonospora* genome) enabled both structural and genomic comparisons to other anthracycline-producing systems informing efforts to characterize keyicin. The new NP was found to be selectively active against Gram-positive bacteria including both *Rhodococcus* sp. and *Mycobacterium* sp. *E. coli*-based chemical genomics studies revealed that keyicin's MOA, in contrast to many other anthracyclines, does not invoke nucleic acid damage.

Graphical abstract

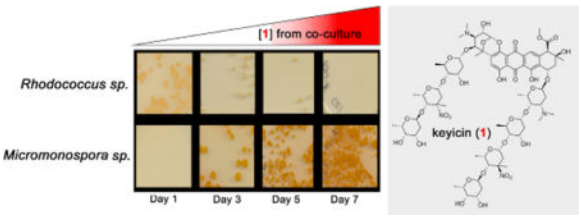

INTRODUCTION

It is now widely recognized that humanity faces a host of burgeoning crises likely to impact global health in the foreseeable future. Principal among these has been the rise of drug resistant microbes set forth, in part, by a loss of interest in natural products (NPs) in the 70s through to the early 2000s across both academia and industry. This change in attitude was inspired by two critical thoughts at the time: **i)** the belief that NP structural diversity and microbial diversities had largely been exhausted, and **ii)** that a more efficient means of identifying drugs and drug leads lay in the prodigious application of combinatorial chemistry and high throughput screening (HTS) technologies. However, our view of drug discovery today is informed largely by technological advances and discoveries over the last 10–20 years that dramatically refute those early tenets and argue that natural products remain one of the greatest sources of molecular diversity applicable to treating human diseases.[1] Revolutionary advances in genome sequencing, proteomics, metabolomics, and other methodologies have changed not only how we see the natural world but also how we can harness its intricacies. The rise of these technologies enabled by technical advances (e.g. those related to nucleic acid and/or protein sequencing and synthesis, mass spectrometry and other diagnostics) as well as dramatic increases in computational capabilities have brought about stunning revelations about microbial diversity and how this influences NP production.[2-16] Microbes leverage NPs to interact with their biotic and abiotic environments and, as such, these metabolites have been selected through evolution for biological relevance, often serving as attractive new drug leads.[17-19] Rational discovery strategies with multidisciplinary approaches can be employed to uncover these bioactive molecules at scale.

For over 80 years, culturable microorganisms formed the basis for NP drug discovery providing unique compounds with useful biological activities and medical uses.[1, 20] Metagenomic studies of the last 10–15 years have shown, however, that the overwhelming majority of microorganisms (> 95%) on earth have either eluded interrogation for NP

Author Manuscript Author Manuscript Author Manuscript Author Manuscript

production, harbor NP biosynthetic gene clusters (BGCs) that remain silent under laboratory culturing conditions, or have been studied using technologies that, at the time, failed to meet the challenges of the day.[21-23] It is believed that only 0.1-1% of the microorganisms on earth have been successfully cultured in the laboratory.[23] At the same time it is now thought that earth harbors ~ 8.7 million eukaryotic species of which about 2.2 million are marine. Similarly, a lower bound of ~ 10000 prokaryotic species of which ~ 1300 are marine has been postulated.[24] However, microbial diversity assessments employing cultivation-independent technologies suggest that these numbers are likely off by ~ 100 fold.[25] For instance, work carried out in support of the International Census of Marine Microbes (ICoMM) initiative has shown that, on average, 1 L of seawater contains 10^8–10^9 bacteria representing ~ 20000 bacterial species.[25]

Especially with respect to prokaryotic species and lower eukaryotes, many of these organisms have proven rich sources of NPs (bacteria, fungi, plants, etc.). Yet it is clear that their molecular diversity, especially in light of what we are now learning about microbiomes and symbiotic relationships, remains dramatically underutilized.[26] Genomics has revealed that the untapped microbial diversity available for drug and drug lead identification efforts far exceeds previous expectations.[1, 22]

Genome mining using biosynthetic signatures from established BGCs has proven to be an important tool in the search for new antimicrobial NPs which has inspired an explosion in BGC sequencing efforts and reported NP-encoding genomes.[7, 15, 27-30] However, identifying new NPs on the basis of BGC mining remains a daunting task; **i)** one genome can house multiple, often dozens of BGCs (of the same, or different classes), **ii)** BGCs might be composed of elements distributed over multiple contigs and may contain genes for which no clear function exists thereby confounding gene-to-reaction correlations, **iii)** identified cryptic BGCs may fail to translate to detectable NPs, **iv)** many microorganisms are recalcitrant to necessary manipulations, and **v)** metagenomic library expression systems are often impractical.[27] Hence, genomic approaches, although an excellent way to identify BGCs and their putative products, are, in the absence of other complementary technologies, insufficient to achieve broadly successful bioinformatics-guided NP identification goals for some biosynthetic classes.[31, 32] However, when used in combination with proteomics and metabolomics, genomics becomes an increasingly powerful tool linking molecules with their biosynthetic genes. It is becoming increasingly evident that by triangulating genomic, proteomic and metabolomic information for microorganisms one becomes better able to address two key questions in current natural products chemistry: **i)** How does one identify interesting organisms when it comes to antimicrobial NP biosynthesis, and **ii)** How can cryptic BGCs be activated in an otherwise unproductive organism? Interdisciplinary approaches have vastly improved the ability to elucidate biosynthetic potentials; especially those that incorporate biological hypotheses in unveiling novel chemistry.[33] Additionally, chemical genomics (CG) now enables one to rapidly gain insight into a NP's mechanism of action further supporting the notion that biological insight hastens chemical discoveries and can drive chemical initiatives.[34] Conclusively linking a BGC to a NP of interest via genome mining-based approaches remains a challenge. However, recent disclosures including the

Author Manuscript Author Manuscript Author Manuscript Author Manuscript

efforts detailed here, highlight that genomics, proteomics and metabolomics can be very effectively leveraged to identify novel producers of unique bioactive NPs.

We report herein the discovery of keyicin (**1**, Figure 1), a novel polynitroglycosylated anthracycline antibiotic, along with early efforts to understand its biosynthesis and mechanism/s of biological activity. An otherwise cryptic NP, keyicin production results from co-culturing of the producer *Micromonospora* strain with *Rhodococcus*. Only through the application and synergy of the technologies noted above was the identification and characterization of **1** possible. Closely related NPs have been identified before but never as the products of co-cultured microbes nor with zwitterionic nitroglycans appended to the aglycone core. Moreover, a great number of such keyicin-like agents have been shown to express biological activities through DNA-dependent means; results of chemical genomics suggest that keyicin functions in a unique manner that is independent of DNA damage processes. We postulate that keyicin is involved in microbial interactions between the co-cultured microbes and that these interactions are representative of similar NP-mediated microbial interactions ubiquitous in nature.[35]

RESULTS AND DISCUSSION

Detection of New Antibiotic via Interspecies Interactions

We have previously developed a microscale co-culturing platform to investigate interspecies interactions between marine invertebrate-associated bacteria with a special emphasis on both genomics and metabolomics.[36] Notably, during the course of co-culturing *Mycobacterium* sp. with *Micromonospora* WMMB-235, *Mycobacterium* inhibition became evident over time. Co-culture-derived antimicrobial activities were selective against the $Gram^+$ bacteria *Bacillus subtilis* and methicillin-sensitive *Staphylococcus aureus* as well as *Mycobacterium* sp. and *Rhodococcus* sp. Notably, all co-culture systems were characterized by a dark red pigmentation that was absent in corresponding monocultures and, of the co-culture systems investigated, the *Micromonospora– Rhodococcus* system generated the largest zone of inhibition. Consequently, the *Micromonospora–Rhodococcus* co-culture system was selected for subsequent metabolomics analysis.

We applied a self-generated in-house LCMS-based metabolomics platform to compare metabolite production between co-cultures and monocultures.[36, 37] Initial fluctuations in LCMS analyses in replicate co-cultures and monocultures were postulated to arise from variable cell concentrations within the seed cultures used to inoculate co-cultures. To alleviate such variances, five seed cultures were inoculated and combined (instead of one culture) prior to co-culturing (see Methods). Repeated microscale co-cultures, using this improved inoculation approach, were evaluated by LCMS-Principal Component Analysis (PCA) metabolomics (Figure 2).[36] In the scores plot, spatial separations of metabolites produced in co-culture versus monoculture extracts were observed. Individual metabolites responsible for observed variances were clearly depicted in the loadings plot. Each symbol in the loadings plot corresponds to a retention time (RT)-mass-to-charge (*m/z*) pair. Compounds clustered in the center of the loadings plot were present in all three strains, while compounds diverging from the cluster represent uniquely produced metabolites.

Author Manuscript Author Manuscript Author Manuscript Author Manuscript

Notably, several compounds were identified as being exclusively produced in co-culture (Figure 2).

Having identified the metabolite likely driving co-culture antimicrobial activity, we carried out bioactivity-guided fractionation of the co-culture extract. A series of related doubly-charged ions $[M + 2H]^{2+}$ = 790.3625, 797.3521 and 805.3524 amu likely correlating to the antimicrobial species was observed and extracted ion chromatograms for each mass confirmed that species production was exclusive to the *Micromonospora–Rhodococcus* co-culture (Supporting Information, Figures S1, S2). Dereplication concerns dictated that all three masses be queried against the Antibase NP database. The co-culture specific species, on the basis of these early efforts, appeared to be previously unreported thus confirming the presumed need to generate keyicin on a scale compatible with complete structural elucidation efforts.

To support structural and mechanistic elucidation efforts both microscale (500 μL) and standard scale (100 mL) fermentations were carried out and sampled daily over a 14 d period.[36] On the basis of LC/MS analyses, keyicin was confirmed to be produced exclusively in co-culture regardless of fermentation scale (see Supporting Information) although microscale fermentations afforded keyicin with reduced rates relative to standard scale fermentations. On the basis of these findings, subsequent fermentations were carried out for 14 d. Before transitioning to large scale fermentations, a media study was carried out using four media: ASW-A [20 g soluble starch, 10 g glucose, 5 g peptone, 5 g yeast extract, 5 g $CaCO_3$ in 1 L artificial seawater (ASW)], ASW-D (2 g yeast extract, 5 g malt extract and 2 g dextrose in 1 L ASW), ISP2 (4 g yeast extract, 10 g malt extract and 4 g dextrose in 1 L ASW) and M1 (10 g soluble starch, 4 g yeast extract, 2 g peptone, 15 g agar in 1 L ASW). LC/MS analyses indicated that nutrient limited ASW-D media produced the highest yields of keyicin. Hence, large scale co-cultures of *Micromonospora* and *Rhodococcus* were carried out for 14 d using ASW-D media enabling sufficient quantities of keyicin to be generated.

Complementary to structure elucidation efforts we also sought to understand the nature of keyicin induction in co-culture. Inspired by earlier reports that NP production in co-cultures of Actinobacteria and mycolic acid-containing bacteria required physical contact between cell types, we endeavored specifically to determine if keyicin biosynthesis might be triggered by physical cell–cell contact.[38] Employing customized growth flasks separated with a 0.2 μm diffusible membrane monocultures of the *Micromonospora* sp. WMMB-235 and *Rhodococcus sp.* were cultured on either side of the membrane (Figure 3). Daily sampling, plating onto agar and incubation revealed that **i)** indeed, neither cell type could traverse the 0.2 μm membrane, and **ii)** over the course of 7 d the growth of the *Micromonospora* sp. remained relatively consistent whereas the *Rhodococcus* sp. suffered significant growth inhibition (Figure 3). Most importantly, production of keyicin was observed by LC/MS. Not surprisingly, disc diffusion of keyicin onto lawns of the *Rhodococcus* sp. or *Mycobacterium* sp. WMMA-183 revealed this compound's antibacterial activity thereby supporting our early observations of growth inhibition during microscale co-cultures. On the basis of these findings it was clear that keyicin biosynthesis does not require

Author Manuscript Author Manuscript Author Manuscript Author Manuscript

physical interactions between the *Rhodococcus* "inducing cells" and the putative *Micromonospora* sp. producer of **1**.

Characterization of the keyicin scaffold

FTICR MS analysis of keyicin (**1**) revealed its molecular formula to be $C_{75}H_{108}N_4O_{34}$ via isotopic fine structure analysis and its 2D structure was determined on the basis of extensive ^{1}H and ^{13}C NMR data sets (Supporting Information). Analysis of ^{13}C NMR data and the red pigment suggested a sp^2 hybridized conjugated carbon skeleton, but only a single aromatic proton, H-3, was observed by ^{1}H NMR. Additionally, the number of ^{13}C resonances did not match the molecular formula. Only after isotopic labeling with ^{13}C-glucose were all resonances detected. We hypothesize that dynamics on the NMR time scale caused severe broadening of H-11 and affected ^{13}C acquisition in the absence of ^{13}C isotopic labeling. Another potentially confounding feature of keyicin was the presence of eight anomeric protons suggesting a multiply glycosylated aglycone. Given this complexity, it was no surprise that classical 2D NMR experiments, including COSY, HSQC and HMBC experiments failed to shed much insight into the structure of the keyicin aglycone.

^{13}C Isotopic incorporation was evaluated with the goal in mind of executing ^{13}C–^{13}C COSY experiments; these would enable us to confidently assign the ^{13}C–^{13}C spin system.[7] Optimized ^{13}C incorporation conditions were identified (Supporting Information, Table S2, Figure S5) enabling extensive use of COSY, HMBC and ROESY approaches to solve the structure of **1**.

Analysis of the ^{13}C–^{13}C COSY data allowed for rapid characterization of the polycyclic phenolic aglycone. Furthermore, the ^{13}C–^{13}C COSY and extensive 1D and 2D NMR data enabled characterization of the eight sugar moieties. The position of H-3 was confirmed using HMBC correlations to C-4a, C-4, C-4′, and C-5′. The C–C spin system beginning with the attachment between C-2 and C-5′, along with HMBC correlation from H-3 to C-4′ and C-5′, indicated a sugar moiety fused to the aglycone. Glycosidic linkages were determined using a combination of HMBC and ROESY correlations to complete the 2D structure of **1** (Figure 4 and Supporting Information).

Strikingly, elucidation of the 2D structure of **1** revealed remarkable similarities, especially with respect to keyicin's aglycone core scaffold, to a number of other NPs whose biosynthetic origins and biological activities are well established. These similarities, especially between the keyicin aglycone, nogalamycin and aclacinomycin A (Figure 5), would come to greatly expedite our efforts to understand the structure and biosynthetic origins of cryptically-encoded NP **1**.

The structural relatedness of keyicin and nogalamycin aglycones proved instrumental in establishing the relative configuration of **1**. Comparisons of ^{13}C shifts for keyicin to those previously established for anthracyclines like aclacinomycin A, arugomycin (AGM) and viriplanin A proved instrumental also in elucidating the structures of sugars S1–S7 (Figure 4 for sugar numbering) as did careful evaluation of HMBC and ROESY correlations (Supporting Information Table S1 and Supporting Experimentals). Moreover, S1–S7 were subjected to conformer distribution analyses using Spartan '14 and conformers with a

Author Manuscript Author Manuscript Author Manuscript Author Manuscript

Boltzmann distribution ≥5% were subjected to geometry optimization and ^{13}C NMR calculations.[39] Calculated carbon chemical shifts were compared to experimental values using the DP4 probability method and the results of these comparisons used to support or refute configurational assignments made on the basis of ^{13}C chemical shift comparisons to known anthracyclines (see Supporting Information).[40] For the more rigid keyicin aglycone, carbon chemical shifts were calculated using an equilibrium conformer followed by geometry optimization and ^{13}C NMR calculations. Despite the smaller difference between calculated and experimental carbon chemical shifts (Δ) for anthraquinone structure **6** versus **5** (Figure 6), DP4 calculations indicated **5** to be slightly favored over **6** (see Supporting Information Figure S20 for complete analysis).

However, comparisons of the methyl C-13 chemical shift for similar anthracyclines including nogalamycin (**3**) AGM,[41, 42] and viriplanin A[43] suggested that the methyl C-13 was on the opposite side of the plane relative to the C-10 pendant carboxymethyl moiety. Consequently, the keyicin A-ring stereochemistry was ultimately assigned as shown by **6** (see Supporting Information).

Elucidation of keyicin's C1′–C6′ fragment also relied heavily upon comparisons to known anthracyclines. Well established AGM and viriplanins as well as keyicin, all belong to the nogalamycin class of anthracyclines; a key differentiating feature is that nogalamycin itself (**3**) bears only a pendant OH moiety at C4′ site whereas all other members of the class bear O-trisaccharide linkages to C4′. This structural feature of **3** versus all other known members of the nogalamycin class proved instrumental in assigning the C4′ configuration of keyicin.

Comparisons of ^{13}C chemical shifts for C1′–C6′ of the noted anthracyclines suggested identical stereochemistry among the molecules; a notable exception being the *R*-configuration and absence of sugar substitution at C4′ for **3**. Given the high degree of structural similarity between AGM and keyicin we paid special attention to the ^{13}C shifts for C3′–C6′ keeping in mind the influence that C4′ configuration would have on the surrounding centers. For AGM these values (C3′ = 62.5, C4′ = 81.6, C5′ = 77.6, C6′ = 23.6 ppm) aligned extremely well with those observed for keyicin (C3′ = 62.7, C4′ = 82.5, C5′ = 78.2, C6′ = 24.2 ppm). In addition, the C3′ pendant N-CH_3 resonances for AGM and keyicin at 44.3 and 44.6 ppm, respectively, strongly supported identical C4′ configurations. Given their putatively identical aglycone configuration, AGM served, in comparisons to **3**, as an effective proxy for keyicin. Accordingly, ^{13}C shift differences for C4′ as well as each compounds proximal N-CH_3 and C6′ carbon suggested different C4′ configuration between nogalamycin and AGM, and by default, keyicin; differences of 2.4, 1.7 and 1.6 ppm were noted for C4′, N-CH_3, and C6′, respectively. These data firmly supported the hypothesis that the aglycones of AGM and keyicin share identical configuration.

That keyicin shares the C4′ *S*-configuration previously demonstrated for AGM and related C4′-glycosylated members of the nogalamycin class was further validated by ROESY. Having defined the relative configuration of all stereocenters in S1 on the basis of ROESY correlations (Supporting Information) we noted a clear ROESY correlation between a C3′ pendant dimethylamine CH_3 and the axial anomeric H of S1. This correlation was consistent

Author Manuscript Author Manuscript Author Manuscript Author Manuscript

with a *syn* placement of H3′ and H4′ of the C1′–C6′ tetrahydropyran moiety and ultimate assignment of the *S*-configuration to the keyicin C4′.

Enzymatic studies with **3** have indicated that two enzymes, SnoK and SnoN, are responsible, respectively, for **i)** installing the C2–C5′ bond resulting in carbocyclization, and **ii)** an epimerization at nogalamycin's C4′ position.[44] Notably, genomic analyses of the keyicin biosynthetic pathway (discussed below) revealed the presence of both *snoK* and *snoN* homologs. Thus, the difference in C4′ configurations between nogalamycin and keyicin may be related to the presence of keyicin's C4′ tethered sugar moiety. We posit that the relative absence of substantive functionality appended to the nogalamycin C4′ enables SnoN-catalyzed epimerization. Conversely, SnoN homologs in the keyicin (and possibly other anthracycline) pathways, may not have C4′ access sufficient to permit epimerization.

Having elucidated the structure of **1**, it becomes apparent that a number of interesting features differentiate keyicin from all other related anthracyclines: **i**) one of the two polysaccharides projected from the aglycone likely assumes a zwitterionic form under physiologically relevant conditions, and **ii**) its construction requires co-culture conditions implying that it plays an important and tunable role in bacterial competition/defensive processes; to date there is no evidence to suggest that other related anthracyclines play as important a role in competitive microbe-microbe associations.

Proteomics Analysis of Keyicin-producing Co-culture and Biosynthetic Insights

Early efforts strongly suggested the *Micromonospora* sp. as the source of **1** in co-cultures and indeed, sequencing of its genome revealed BGCs representative of one type I polyketide synthase (PKS), two type II PKSs, one type III PKS, one lanthipeptide and six hybrid clusters.[45] Also notable were *ORFs* encoding seven glycosyltransferases (GTs) associated with S1–S7; further functional annotations within the putative keyicin BGC (Supporting Information, Tables S3, S4) further implicated the *Micromonospora* sp. as the producer of **1** in co-culture. Sequencing of the *Rhodococcus* sp. genome[46] on the other hand, failed to reveal any evidence of type II PKS *ORFs*.

With this genomic information in hand we carried out proteomic analyses of *Micromonospora–Rhodococcus* co-cultures and monocultures targeting only large proteins for identification; all significant proteins (or fragments thereof) were identified using PEAKS[47] software and imported raw LC-MS/MS data were used to search the annotated *Micromonospora* sp. and *Rhodococcus* sp. genomes[45, 46] Five proteins associated with keyicin construction were identified in both co-culture and *Micromonospora* sp. monoculture. Putative generic cyclase (Kyc9), dTDP-4-dehydrorhamnose 3,5-epimerase (Kyc28) and PKS cyclase (Kyc34) enzymes were detected in biological triplicate analyses as were a phytanoyl-CoA dioxygenase (product of *kyc17*) and a 3-oxoacyl-(acyl-carrier protein). Significantly, all five *Micromonospora*-derived enzymes predicted during early genomics efforts and a DUF4440 domain-containing protein (termed Kyc51) were identified in all co-culture replicates, but in only one replicate of the *Micromonospora* sp. monoculture suggesting that, when confronted with the *Rhodococcus*-specific components (as during co-cultures), the *Micromonospora* sp. amplifies expression of specific biosynthetic proteins associated with keyicin production.

Author Manuscript Author Manuscript Author Manuscript Author Manuscript

Anthracycline BGCs and Structures Illuminate Keyicin Construction

Genomics data for both co-culture organisms[45, 46] allow us to glean significant biosynthetic and structural insights far exceeding our assignment of the *Micromonospora* sp. as the induced manufacturer of **1**. Indeed, these data provide significant validation of the proteomics information enabling assignment of keyicin biosynthesis to the *Micromonospora* sp. rather than the *Rhodococcus* strain. In addition to having aided the structural characterization of keyicin, nogalamycin (MIBiG: BGC0000250) and aclacinomycin A (MIBiG: BGC0000191→BGC0000193) again serve as important reference points by way of their well-established biosynthetic gene clusters. The high degree of structural and genetic similarity between the keyicin and nogalamycin systems provide further validation, not only of the keyicin producer assignment but also key structural assignments for keyicin.

Of interest were genes located within each BGC that code for highly specific, and unique functionalities that define the shared keyicin/nogalamycin benzoxocin scaffold as highlighted in Figure 7. Review of the BGCs for both natural products revealed well over 30 genes across both systems that share > 60% similarity (Supporting Information, Table S3); the most interesting of these relate to benzoxocin construction. It is now well established that the products of *snoaL2* and *snoaW* hydroxylate the C-1 of a nogalamycinone intermediate[48, 49] followed by glycosylation of the newly installed phenol with nogalamine by SnogD[50] and that the redox enzyme SnoK[44] carries out C–C bond formation linking the C5′ of the newly installed nogalamine *ortho* to the newly generated aryl ether linkage. Genes within the *kyc* cluster responsible for this same sequence of transformations are *kyc36/kyc51* followed by *kyc52* (glycolase) and *kyc17*, respectively (Figure 7). The structural assignments made in advance of BGC studies are strongly supported by these genomic data.

In addition to genes dictating benzoxocin construction in both BGCs, a great many other genes have been identified within the *kyc* cluster showing strong similarity/homology to nogalamycin cluster components. A handful of these critical putative homologs are indicated in Table 1.

The benzoxocin moieties of keyicin and nogalamycin differentiate these species from the overwhelming majority of other anthracyclines. Even between keyicin and nogalamycin however, an important differentiation is observed beyond the benzoxocin scaffold. SnoN (encoded within the nogalamycin cluster) is responsible for setting the C4′ configuration of nogalamycin via epimerization.[44] Within the *kyc* cluster, *kyc54* codes for a highly similar enzyme (71% similarity, Table 1) yet the C4′ configuration in keyicin is inverted relative to that in nogalamycin. In considering the origins of this stereochemical difference we posit that the presence of the pendant trisaccharide at C4′ in keyicin likely prohibits Kyc54-promoted epimerization. Devoid of any similar steric encumbrance, SnoN is presumably highly efficient at processing the less heavily glycosylated nogalamycin intermediate. Thus, we propose that the pendant C4′-linked sugar in keyicin prohibits Kyc54 action. This is interesting not only in the context of contrasting the keyicin and nogalamycin systems but also because it suggests that C4′ epimerization in each pathway comes at a very late stage during biosynthesis and is presumably a “post-tailoring” step; it is rare that an aglycone is

Author Manuscript Author Manuscript Author Manuscript Author Manuscript

subject to post-tailoring modifications. The data observed here however, suggests that the keycin/nogalamycin systems may be one such representative.

In addition to clear similarities between the nogalamycin and keyicin scaffolds and BGCs MIBiG accession numbers identified using antiSMASH revealed often dramatic genetic similarity to BGCs for other anthracycline natural products. The keyicin BGC was found to have very highly shared gene content to the BGCs for cinerubin B (MIBiG: BGC0000212, 88%), cosmomycin D (MIBiG: BGC0001074, 88%), arimetamycin (MIBiG: BGC0000199, 84%), kosinostatin (MIBiG: BGC0001073, 75%), aclacinomycin (MIBiG: BGC0000191, 72%) (Supporting Information, Table S5, Figure S21 for relevant structures). To put these data into context, it is instructive to note that the BGCs for keyicin and nogalamycin (MIBiG: BGC0000250) display 52% overall similarity.

A-ring glycosylation during keyicin construction provides yet another opportunity to correlate features of the *kyc* BGC to those of other, more well-established anthracycline BGCs. During aclacinomycin construction the enzyme duo of AknS and AknT employs TDP-l-rhodosamine to tether a rhodosamine sugar to the precursor aklavinone C7-OH moiety.[56] AknK then employs TDP-2-deoxy-l-fucose to glycosylate the newly added rhodosamine moiety.[57] The resulting disaccharide can undergo another cycle of glycosylation at the hands of AknK to render the final trisaccharide.[57] Notably, within the cosmomyin D cluster, *cosK* displays 79% similarity to *aknK* and has been shown experimentally to carry out the same transformation during cosmomycin D construction as that of AknK during aclacinomycin A production.[58] Like aclacinomycin, cosmomycin D production calls for C7-OH glycosylation with L-rhodosamine. This transformation is carried out by CosG which transfers rhodosamine to both the 7- and 10-positions of the cosmomycin aglycone; the C7-OH tethered species then serves as a substrate for fucosylation by CosK *en route* to the final trisaccharide that distinguishes this species from other members of the cosmomycin family.[58] Not surprisingly, the *kyc* cluster contains three genes with moderate to good similarities to the GTs noted above; SEARCHGTr software further supported early hypotheses correlating specific chemistries to *kyc* genes.[59] For rhodosamine transfer, *kyc26* displays 43% similarity to AknT (AAF73456.1) and *kyc25* shows 56% similarity to AknS (AAF73455.1); with regard to the cosmomycin system, *kyc25* shows 60% similarity to CosG (KDN80069.1). In considering fucose transfer, AknK appears to have a number of candidate homologs within the *kyc* cluster; these genes, with accompanying similarities to AknK, include *kyc12* (48.5%), *kyc20* (52%), *kyc24* (53%), *kyc29* (50%), *kyc32* (47.7%) and *kyc52* (30%). The application of SEARCHGTr, a program specifically designed for GT analysis that takes into consideration donor and recipient active site architectures further supported the notion that GTs involved in keyicin construction bear similarity to other more well-established GTs (Supporting Information, Table S4).[59] Not surprisingly, the same *kyc* genes, with the exception of *kyc52*, with similarity to AknK also prove similar to CosK. Putative CosK homolog candidates include the keyicin biosynthetic products of *kyc12* (49.8%), *kyc20* (54%), *kyc24* (55%), *kyc29* (27.4%), and *kyc32* (48.8%). Consequently, many elements within the *kyc* BGC correlate both keyicin structural and genomics features to those of other closely related anthracyclines (Supporting Information, Table S5). These strong associations across compounds and their microbial producers

Author Manuscript Author Manuscript Author Manuscript Author Manuscript

provide strong support for our structural elucidation of keyicin and illuminate opportunities for potential biosynthetic engineering efforts.

Biological Activity of Keyicin

Keyicin (**1**) was screened against both Gram-positive and Gram-negative bacteria. Similar to the observed antibiotic activity of the crude extracts, keyicin exhibited selective Gram-positive activity. In addition to the growth inhibition of *Mycobacterium* sp. and *Rhodococcus* sp., keyicin inhibited *B. subtilis* and Methicillin-sensitive *Staphylococcus aureus* (MSSA) at minimum inhibitory concentrations (MICs) of 8 μg/mL (9.9 μM) and 2 μg/mL (2.5 μM), respectively.

Chemical Genomics Shed Insight into Key-icin Mechanism of Action

Chemical genomics (CG) provides a means of rapidly and comprehensively assessing the pathways and processes that underlie cellular vulnerabilities to small molecules. Likewise, CG can also give insight into mechanisms of cellular resistance to such agents. We employed CG to gain broad insight into keyicin's biological mode of action. Specifically we assessed the ability of keyicin, like other anthracyclines, to induce DNA damage as reflected by downstream effects.[60-62] Cells bearing mutations that impair the ability to sustain DNA damage are more susceptible to DNA damaging agents than are those with intact compensatory mechanisms. Accordingly, we treated a barcoded *E. coli* deletion collection with keyicin (12.5 μg/mL) and compared the resulting CG profile with those obtained from cells exposed to the well-established DNA-intercalator ethidium bromide (100 μg/mL), and methyl methanesulfonate (MMS, 0.0125%), a known DNA alkylating/damaging agent. The CG profile of keyicin was distinct from EtBr and MMS (Supporting Information, Figure S22); The profiles of EtBr and MMS had a correlation coefficient of 0.47. Keyicin, on the other hand, had a correlation of 0.11 with EtBr and 0.16 with MMS. Particularly telling was that cells bearing inactivations of *recA*, a key gene involved in DNA repair in *E. coli* and established indicator of DNA damaging agents,[63] proved particularly susceptible to the effects of EtBr and MMS yet were essentially unaffected by keyicin (Supporting Information for detailed data analysis).

Among the 20 *E. coli* mutants most sensitive to keyicin, not a single one is involved in DNA replication or repair machineries, strongly suggesting that keyicin's principal mode of action does not involve DNA damage. In fact, in considering the 46 gene mutants with significant sensitivities to keyicin (Supporting Information, Table S7). no clear and significant functional enrichment is apparent to help illuminate keyicin's mode of action. Evaluations of the network around these 46 genes suggest, tentatively, that keyicin may exert antibacterial activity through modulation of fatty acid metabolism (Supporting Information). Consequently, investigations of keyicin's impact on bacterial lipid metabolism, as expeditiously brought to light by these CG studies, are clearly warranted.

Conclusions

The advent of interdisciplinary omics technologies has made clear that cryptic biosynthetic gene clusters encode for a significant number of, as yet unknown, but potentially promising

Author Manuscript Author Manuscript Author Manuscript Author Manuscript

antibiotics. We previously developed an approach to investigate the secondary metabolite induction resulting from interspecies interactions. Using this approach, a *Rhodococcus* sp. was found to induce production of a new antibiotic, keyicin, when co-cultured with *Micromonospora* sp. Structure elucidation of keyicin was assisted by 2D ^{13}C NMR and informed, in part, by comparisons of key elements of its BGC with those of structurally related and biosynthetically characterized anthracyclines. Production of keyicin was not dependent on direct cell-cell contact, which contradicts previous reports of secondary metabolite induction by mycolic acid-containing bacteria. Keyicin was selectively active against Gram-positive bacteria including both *Rhodococcus* sp. and *Mycobacterium* sp. The *E coli* chemical genomics provided encouraging results surrounding a putative unique MOA for keyicin, and importantly, one that does not involve DNA damage.

METHODS

See the Supporting Information for details.

Supplementary Material

Refer to Web version on PubMed Central for supplementary material.

Acknowledgments

This work was supported by funding from the University of Wisconsin-Madison School of Pharmacy and from the University of Wisconsin Institute for Clinical and Translational Research funded through NIH/NCATS UL1TR000427. This work was also funded by the NIH through the administration of NIGMS Grants R01GM104192 (T.S.B.) and R01GM104975 (to C.L.M), NIDDK R01DK071801 (to L.L.), HGRI grants R01HG005084 (to C.L.M) and 1R01HG0050 (to C.L.M. & J.S.P.) as well as U19-Al109673 (to C.R.C.). NIH Biotechnology training grants T32GM008347 (to S.W.S.) and T32GM008505 (to M.C.) are also gratefully acknowledged; S.W.S. is also supported by an NSF Graduate Research Fellowship (00039202). We thank the Analytical Instrumentation Center at the University of Wisconsin-Madison for the facilities to acquire spectroscopic data. Orbitrap instruments were purchased through the support of an NIH shared instrument grant (NIH-NCRR S10RR029531 to L.L.) and the Office of the Vice Chancellor for Research and Graduate Education at the University of Wisconsin-Madison. This study made use of the National Magnetic Resonance Facility at Madison (NMRFAM), which is supported by NIH grant P41GM103399. Additional equipment was purchased with funds from the University of Wisconsin, the NIH (RR02781, RR08438), the NSF (DMB-8415048, OIA-9977486, BIR-9214394), and the USDA. L.L. acknowledges a Vilas Distinguished Achievement Professorship and a Janis Apinis Profes sorship with funding provided by the Wisconsin Alumni Research Foundation and University of Wisconsin-Madison School of Pharmacy. We also thank D. Demaria for assistance with sample collection and express our appreciation to H. Mori (Nara Institute of Science and Technology, Ikoma, Japan) for generous provision of the barcoded *E. coli* deletion collection.

References

1. Pye CR, Bertin MJ, Lokey RS, Gerwick WH, Linington RG. Retrospective analysis of natural products provides insights for future discovery trends. Proc Natl Acad Sci U S A. 2017; 114:5601–5606. [PubMed: 28461474]
2. Yuet KP, Tirrell DA. Chemical tools for temporally and spatially resolved mass spectrometry-based proteomics. Ann Biomed Eng. 2014; 42:299–311. [PubMed: 23943069]
3. Yang JY, Sanchez LM, Rath CM, Liu X, Boudreau PD, Bruns N, Glukhov E, Wodtke A, de Felicio R, Fenner A, Wong WR, Linington RG, Zhang L, Debonsi HM, Gerwick WH, Dorrestein PC. Molecular networking as a dereplication strategy. J Nat Prod. 2013; 76:1686–1699. [PubMed: 24025162]
4. Watrous J, Roach P, Alexandrov T, Heath BS, Yang JY, Kersten RD, van der Voort M, Pogliano K, Gross H, Raaijmakers JM, Moore BS, Laskin J, Bandeira N, Dorrestein PC. Mass spectral

Author Manuscript Author Manuscript Author Manuscript Author Manuscript

molecular networking of living microbial colonies. Proc Natl Acad Sci U S A. 2012; 109:E1743–1752. [PubMed: 22586093]

5. Shih CJ, Chen PY, Liaw CC, Lai YM, Yang YL. Bringing microbial interactions to light using imaging mass spectrometry. Nat Prod Rep. 2014; 31:739–755. [PubMed: 24452118]
6. Quinn RA, Nothias LF, Vining O, Meehan M, Esquenazi E, Dorrestein PC. Molecular Networking As a Drug Discovery, Drug Metabolism, and Precision Medicine Strategy. Trends Pharmacol Sci. 2017; 38:143–154. [PubMed: 27842887]
7. Mohimani H, Kersten RD, Liu WT, Wang M, Purvine SO, Wu S, Brewer HM, Pasa-Tolic L, Bandeira N, Moore BS, Pevzner PA, Dorrestein PC. Automated genome mining of ribosomal peptide natural products. ACS Chem Biol. 2014; 9:1545–1551. [PubMed: 24802639]
8. Medema MH, Kottmann R, Yilmaz P, Cummings M, Biggins JB, Blin K, de Bruijn I, Chooi YH, Claesen J, Coates RC, Cruz-Morales P, Duddela S, Dusterhus S, Edwards DJ, Fewer DP, Garg N, Geiger C, Gomez-Escribano JP, Greule A, Hadjithomas M, Haines AS, Helfrich EJ, Hillwig ML, Ishida K, Jones AC, Jones CS, Jungmann K, Kegler C, Kim HU, Kotter P, Krug D, Masschelein J, Melnik AV, Mantovani SM, Monroe EA, Moore M, Moss N, Nutzmann HW, Pan G, Pati A, Petras D, Reen FJ, Rosconi F, Rui Z, Tian Z, Tobias NJ, Tsunematsu Y, Wiemann P, Wyckoff E, Yan X, Yim G, Yu F, Xie Y, Aigle B, Apel AK, Balibar CJ, Balskus EP, Barona-Gomez F, Bechthold A, Bode HB, Borriss R, Brady SF, Brakhage AA, Caffrey P, Cheng YQ, Clardy J, Cox RJ, De Mot R, Donadio S, Donia MS, van der Donk WA, Dorrestein PC, Doyle S, Driessen AJ, Ehling-Schulz M, Entian KD, Fischbach MA, Gerwick L, Gerwick WH, Gross H, Gust B, Hertweck C, Hofte M, Jensen SE, Ju J, Katz L, Kaysser L, Klassen JL, Keller NP, Kormanec J, Kuipers OP, Kuzuyama T, Kyrpides NC, Kwon HJ, Lautru S, Lavigne R, Lee CY, Linquan B, Liu X, Liu W, Luzhetskyy A, Mahmud T, Mast Y, Mendez C, Metsa-Ketela M, Micklefield J, Mitchell DA, Moore BS, Moreira LM, Muller R, Neilan BA, Nett M, Nielsen J, O'Gara F, Oikawa H, Osbourn A, Osburne MS, Ostash B, Payne SM, Pernodet JL, Petricek M, Piel J, Ploux O, Raaijmakers JM, Salas JA, Schmitt EK, Scott B, Seipke RF, Shen B, Sherman DH, Sivonen K, Smanski MJ, Sosio M, Stegmann E, Sussmuth RD, Tahlan K, Thomas CM, Tang Y, Truman AW, Viaud M, Walton JD, Walsh CT, Weber T, van Wezel GP, Wilkinson B, Willey JM, Wohlleben W, Wright GD, Ziemert N, Zhang C, Zotchev SB, Breitling R, Takano E, Glockner FO. Minimum Information about a Biosynthetic Gene cluster. Nat Chem Biol. 2015; 11:625–631. [PubMed: 26284661]
9. Krug D, Muller R. Secondary metabolomics: the impact of mass spectrometry-based approaches on the discovery and characterization of microbial natural products. Nat Prod Rep. 2014; 31:768–783. [PubMed: 24763662]
10. Kersten RD, Yang YL, Xu Y, Cimermancic P, Nam SJ, Fenical W, Fischbach MA, Moore BS, Dorrestein PC. A mass spectrometry-guided genome mining approach for natural product peptidogenomics. Nat Chem Biol. 2011; 7:794–802. [PubMed: 21983601]
11. Goodwin CR, Sherrod SD, Marasco CC, Bachmann BO, Schramm-Sapyta N, Wikswo JP, McLean JA. Phenotypic mapping of metabolic profiles using self-organizing maps of high-dimensional mass spectrometry data. Analytical chemistry. 2014; 86:6563–6571. [PubMed: 24856386]
12. Duncan KR, Crusemann M, Lechner A, Sarkar A, Li J, Ziemert N, Wang M, Bandeira N, Moore BS, Dorrestein PC, Jensen PR. Molecular networking and pattern-based genome mining improves discovery of biosynthetic gene clusters and their products from Salinispora species. Chem Biol. 2015; 22:460–471. [PubMed: 25865308]
13. Covington BC, McLean JA, Bachmann BO. Comparative mass spectrometry-based metabolomics strategies for the investigation of microbial secondary metabolites. Nat Prod Rep. 2017; 34:6–24. [PubMed: 27604382]
14. Barkal LJ, Theberge AB, Guo CJ, Spraker J, Rappert L, Berthier J, Brakke KA, Wang CC, Beebe DJ, Keller NP, Berthier E. Microbial metabolomics in open microscale platforms. Nat Commun. 2016; 7:10610. [PubMed: 26842393]
15. Boddy CN. Bioinformatics tools for genome mining of polyketide and non-ribosomal peptides. J Ind Microbiol Biotechnol. 2014; 41:443–450. [PubMed: 24174214]
16. Chakraborty C, Doss CG, Patra BC, Bandyopadhyay S. DNA barcoding to map the microbial communities: current advances and future directions. Appl Microbiol Biotechnol. 2014; 98:3425–3436. [PubMed: 24522727]

Author Manuscript Author Manuscript Author Manuscript Author Manuscript

17. Walsh CT, Fischbach MA. Natural Products Version 2.0: Connecting Genes to Molecules. Journal of the American Chemical Society. 2010; 132:2469–2493. [PubMed: 20121095]
18. Fischbach MA, Walsh CT, Clardy J. The evolution of gene collectives: How natural selection drives chemical innovation. Proc Natl Acad Sci U S A. 2008; 105:4601–4608. [PubMed: 18216259]
19. Cantley AM, Clardy J. Animals in a bacterial world: opportunities for chemical ecology. Nat Prod Rep. 2015; 32:888–892. [PubMed: 25656944]
20. Stewart EJ. Growing unculturable bacteria. J Bacteriol. 2012; 194:4151–4160. [PubMed: 22661685]
21. Newman DJ. Predominately Uncultured Microbes as Sources of Bioactive Agents. Front Microbiol. 2016; 7:1832. [PubMed: 27917159]
22. Cimermancic P, Medema MH, Claesen J, Kurita K, Wieland Brown LC, Mavrommatis K, Pati A, Godfrey PA, Koehrsen M, Clardy J, Birren BW, Takano E, Sali A, Linington RG, Fischbach MA. Insights into secondary metabolism from a global analysis of prokaryotic biosynthetic gene clusters. Cell. 2014; 158:412–421. [PubMed: 25036635]
23. Katz M, Hover BM, Brady SF. Culture-independent discovery of natural products from soil metagenomes. J Ind Microbiol Biotechnol. 2016; 43:129–141. [PubMed: 26586404]
24. Mora C, Tittensor DP, Adl S, Simpson AG, Worm B. How many species are there on Earth and in the ocean? PLoS Biol. 2011; 9:e1001127. [PubMed: 21886479]
25. Amaral-Zettler, L., Artigas, LF., Baross, J., Bharathi, PAL., Boetius, A., Chandramohan, D., Herndl, G., Kogure, K., Neal, P., Pedrós-Alió, C., Ramette, A., Schouten, S., Stal, L., Thessen, A., Leeuw, Jd, Sogin, M. Life in the World's Oceans. Wiley-Blackwell; 2010. A Global Census of Marine Microbes; p. 221-245.
26. Adnani N, Rajski SR, Bugni TS. Symbiosis-inspired approaches to antibiotic discovery. Nat Prod Rep. 2017; 34:784–814. [PubMed: 28561849]
27. Gubbens J, Zhu H, Girard G, Song L, Florea BI, Aston P, Ichinose K, Filippov DV, Choi YH, Overkleeft HS, Challis GL, van Wezel GP. Natural product proteomining, a quantitative proteomics platform, allows rapid discovery of biosynthetic gene clusters for different classes of natural products. Chem Biol. 2014; 21:707–718. [PubMed: 24816229]
28. Van Lanen SG, Shen B. Microbial genomics for the improvement of natural product discovery. Curr Opin Microbiol. 2006; 9:252–260. [PubMed: 16651020]
29. Micallef ML, D'Agostino PM, Sharma D, Viswanathan R, Moffitt MC. Genome mining for natural product biosynthetic gene clusters in the Subsection V cyanobacteria. BMC Genomics. 2015; 16:669. [PubMed: 26335778]
30. Medema MH, Fischbach MA. Computational approaches to natural product discovery. Nat Chem Biol. 2015; 11:639–648. [PubMed: 26284671]
31. Miller I, Chevrette M, Kwan J. Interpreting Microbial Biosynthesis in the Genomic Age: Biological and Practical Considerations. Marine Drugs. 2017; 15:165.
32. Udwary DW, Zeigler L, Asolkar RN, Singan V, Lapidus A, Fenical W, Jensen PR, Moore BS. Genome sequencing reveals complex secondary metabolome in the marine actinomycete Salinispora tropica. Proc Natl Acad Sci U S A. 2007; 104:10376–10381. [PubMed: 17563368]
33. Florez LV, Biedermann PH, Engl T, Kaltenpoth M. Defensive symbioses of animals with prokaryotic and eukaryotic microorganisms. Nat Prod Rep. 2015; 32:904–936. [PubMed: 25891201]
34. Piotrowski JS, Simpkins SW, Li SC, Deshpande R, McIlwain SJ, Ong IM, Myers CL, Boone C, Andersen RJ. Chemical genomic profiling via barcode sequencing to predict compound mode of action. Methods in Molecular Biology (Clifton, NJ). 2015; 1263:299–318.
35. Clardy J, Fischbach MA, Currie CR. The natural history of antibiotics. Curr Biol. 2009; 19:R437–441. [PubMed: 19515346]
36. Adnani N, Vazquez-Rivera E, Adibhatla SN, Ellis GA, Braun DR, Bugni TS. Investigation of Interspecies Interactions within Marine Micromonosporaceae Using an Improved Co-Culture Approach. Marine drugs. 2015; 13:6082–6098. [PubMed: 26404321]

Author Manuscript Author Manuscript Author Manuscript Author Manuscript

37. Hou Y, Braun DR, Michel CR, Klassen JL, Adnani N, Wyche TP, Bugni TS. Microbial strain prioritization using metabolomics tools for the discovery of natural products. Anal Chem. 2012; 84:4277–4283. [PubMed: 22519562]
38. Onaka H, Mori Y, Igarashi Y, Furumai T. Mycolic acid-containing bacteria induce natural-product biosynthesis in Streptomyces species. Applied and Env Microbiol. 2011; 77:400–406.
39. Shao Y, Molnar LF, Jung Y, Kussmann J, Ochsenfeld C, Brown ST, Gilbert AT, Slipchenko LV, Levchenko SV, O'Neill DP, DiStasio RA Jr, Lochan RC, Wang T, Beran GJ, Besley NA, Herbert JM, Lin CY, Van Voorhis T, Chien SH, Sodt A, Steele RP, Rassolov VA, Maslen PE, Korambath PP, Adamson RD, Austin B, Baker J, Byrd EF, Dachsel H, Doerksen RJ, Dreuw A, Dunietz BD, Dutoi AD, Furlani TR, Gwaltney SR, Heyden A, Hirata S, Hsu CP, Kedziora G, Khalliulin RZ, Klunzinger P, Lee AM, Lee MS, Liang W, Lotan I, Nair N, Peters B, Proynov EI, Pieniazek PA, Rhee YM, Ritchie J, Rosta E, Sherrill CD, Simmonett AC, Subotnik JE, Woodcock HL 3rd, Zhang W, Bell AT, Chakraborty AK, Chipman DM, Keil FJ, Warshel A, Hehre WJ, Schaefer HF 3rd, Kong J, Krylov AI, Gill PM, Head-Gordon M. Advances in methods and algorithms in a modern quantum chemistry program package. Phys Chem Chem Phys. 2006; 8:3172–3191. [PubMed: 16902710]
40. Smith SG, Goodman JM. Assigning stereochemistry to single diastereoisomers by GIAO NMR calculation: the DP4 probability. J Am Chem Soc. 2010; 132:12946–12959. [PubMed: 20795713]
41. Kawai H, Hayakawa Y, Nakagawa M, Furihata K, Seto H, Otake N. Arugomycin, a new anthracycline antibiotic. II. Structural elucidation. J Antibiot (Tokyo). 1987; 40:1273–1282. [PubMed: 3479413]
42. Kawai H, Hayakawa Y, Nakagawa M, Furihata K, Furihata K, Shimazu A, Seto H, Otake N. Arugomycin, a new anthracycline antibiotic. I. Taxonomy, fermentation, isolation and physico-chemical properties. J Antibiot (Tokyo). 1987; 40:1266–1272. [PubMed: 3479412]
43. Hutter K, Baader E, Frobel K, Zeeck A, Bauer K, Gau W, Kurz J, Schroder T, Wunsche C, Karl W, et al. Viriplanin A, a new anthracycline antibiotic of the nogalamycin group. I. Isolation, characterization, degradation reactions and biological properties. J Antibiot (Tokyo). 1986; 39:1193–1204. [PubMed: 3023268]
44. Siitonen V, Selvaraj B, Niiranen L, Lindqvist Y, Schneider G, Metsa-Ketela M. Divergent non-heme iron enzymes in the nogalamycin biosynthetic pathway. Proc Natl Acad Sci U S A. 2016; 113:5251–5256. [PubMed: 27114534]
45. Adnani N, Braun DR, McDonald BR, Chevrette MG, Currie CR, Bugni TS. Draft Genome Sequence of Micromonospora sp. Strain WMMB235, a Marine Ascidian-Associated Bacterium. Genome Announcements. 2017; 5:e01369–16. [PubMed: 28082484]
46. Adnani N, Braun DR, McDonald BR, Chevrette MG, Currie CR, Bugni TS. Complete Genome Sequence of Rhodococcus sp. Strain WMMA185, a Marine Sponge-Associated Bacterium. Genome Announcements. 2016; 4:e01406–16.
47. Ma B, Zhang K, Hendrie C, Liang C, Li M, Doherty-Kirby A, Lajoie G. PEAKS: powerful software for peptide de novo sequencing by tandem mass spectrometry. Rapid communications in mass spectrometry : RCM. 2003; 17:2337–2342. [PubMed: 14558135]
48. Sultana A, Kallio P, Jansson A, Niemi J, Mantsala P, Schneider G. Crystallization and preliminary crystallographic data of SnoaL, a polyketide cyclase in nogalamycin biosynthesis, Acta crystallographica. Section D, Biological crystallography. 2004; 60:1118–1120.
49. Siitonen V, Blauenburg B, Kallio P, Mantsala P, Metsa-Ketela M. Discovery of a two-component monooxygenase SnoaW/SnoaL2 involved in nogalamycin biosynthesis. Chem Biol. 2012; 19:638–646. [PubMed: 22633415]
50. Claesson M, Siitonen V, Dobritzsch D, Metsa-Ketela M, Schneider G. Crystal structure of the glycosyltransferase SnogD from the biosynthetic pathway of nogalamycin in Streptomyces nogalater. FEBS J. 2012; 279:3251–3263. [PubMed: 22804797]
51. Klymyshin D, Stephanyshyn O, Fedorenko V. THE ROLE OF STREPTOMYCES NOGALATER Lv65 *snoaM*, *snoaL* and *snoaE* GENES IN NOGALAMYCIN BIOSYNTHESIS. TSitologiia i genetika. 2015; 49:9–16. [PubMed: 26214900]
52. Siitonen V, Claesson M, Patrikainen P, Aromaa M, Mantsala P, Schneider G, Metsa-Ketela M. Identification of late-stage glycosylation steps in the biosynthetic pathway of the anthracycline nogalamycin. Chembiochem. 2012; 13:120–128. [PubMed: 22120896]

Author Manuscript Author Manuscript Author Manuscript Author Manuscript

53. Shao L, Shi X, Liu W, Gao X, Pu T, Ma B, Wang S. Inactivation and identification of three genes encoding glycosyltransferase required for biosynthesis of nogalamycin. Biotechnol Appl Biochem. 2015; 62:765–771. [PubMed: 25524457]

54. Bechthold A, Yan X. SnoaW/SnoaL2: a different two-component monooxygenase. Chem Biol. 2012; 19:549–551. [PubMed: 22633406]

55. Klimyshin DO, Gren TP, Fedorenko VO. Role of the snorA gene in nogalamycin biosynthesis by strain Streptomyces nogalater Lv65. Mikrobiologiia. 2011; 80:490–495. [PubMed: 22073550]

56. Leimkuhler C, Fridman M, Lupoli T, Walker S, Walsh CT, Kahne D. Characterization of rhodosaminyl transfer by the AknS/AknT glycosylation complex and its use in reconstituting the biosynthetic pathway of aclacinomycin A. J Am Chem Soc. 2007; 129:10546–10550. [PubMed: 17685523]

57. Lu W, Leimkuhler C, Oberthur M, Kahne D, Walsh CT. AknK is an L-2-deoxyfucosyltransferase in the biosynthesis of the anthracycline aclacinomycin A. Biochemistry. 2004; 43:4548–4558. [PubMed: 15078101]

58. Garrido LM, Lombo F, Baig I, Nur EAM, Furlan RL, Borda CC, Brana A, Mendez C, Salas JA, Rohr J, Padilla G. Insights in the glycosylation steps during biosynthesis of the antitumor anthracycline cosmomycin: characterization of two glycosyltransferase genes. Appl Microbiol Biotechnol. 2006; 73:122–131. [PubMed: 16810496]

59. Kamra P, Gokhale RS, Mohanty D. SEARCHGTr: a program for analysis of glycosyltransferases involved in glycosylation of secondary metabolites. Nucleic Acids Res. 2005; 33:W220–225. [PubMed: 15980457]

60. Minotti G, Menna P, Salvatorelli E, Cairo G, Gianni L. Anthracyclines: molecular advances and pharmacologic developments in antitumor activity and cardiotoxicity. Pharmacological reviews. 2004; 56:185–229. [PubMed: 15169927]

61. Kizek R, Adam V, Hrabeta J, Eckschlager T, Smutny S, Burda JV, Frei E, Stiborova M. Anthracyclines and ellipticines as DNA-damaging anticancer drugs: recent advances. Pharmacology & therapeutics. 2012; 133:26–39. [PubMed: 21839775]

62. Gewirtz DA. A critical evaluation of the mechanisms of action proposed for the antitumor effects of the anthracycline antibiotics adriamycin and daunorubicin. Biochem Pharmacol. 1999; 57:727–741. [PubMed: 10075079]

63. Bellou S, Muenter M, Travers M, Leifer B, Baig S, Kramer C, Qi M, Joshi C, Carlson A, Conway C. Determination of Escherichia coli Genes Involved in Resistance to DNA Alkylating Agents. The FASEB Journal. 2016; 30(1 Suppl) 789.3.

Author Manuscript Author Manuscript Author Manuscript Author Manuscript

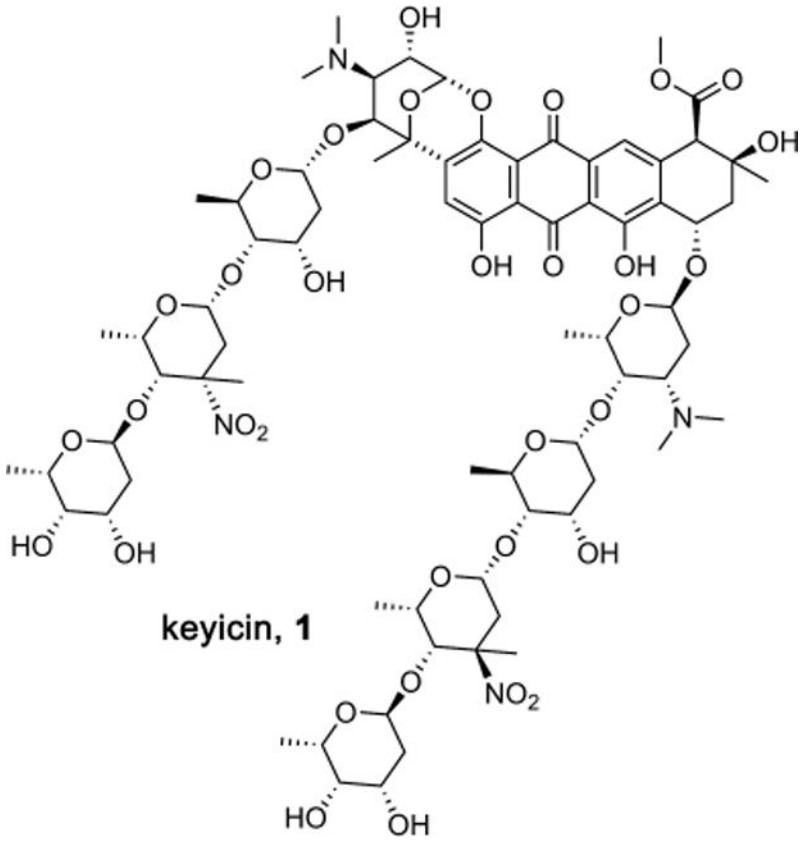

Figure 1.
Structure of new co-culture-dependent antibiotic keyicin (**1**).

Author Manuscript Author Manuscript Author Manuscript Author Manuscript

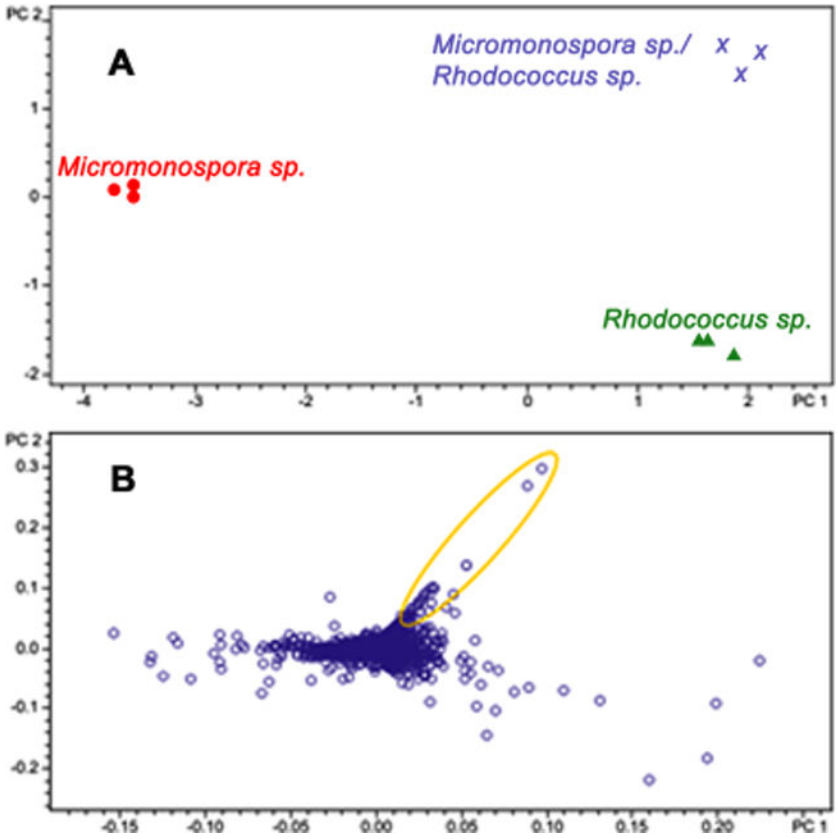

Figure 2.

LCMS-PCA metabolomics of *Micromonospora* sp. and *Rhodococcus* sp. co-culture. (**A**) PCA scores plot describing variance in metabolites in co-culture and monoculture extracts of the *Micromonospora* sp. and *Rhodococcus* sp. (**B**) PCA loadings plot displaying individual metabolites responsible for the variance observed between extracts; the high variance seen in co-culture extracts is attributable to metabolites highlighted by the yellow oval in plot 2B.

Author Manuscript Author Manuscript Author Manuscript Author Manuscript

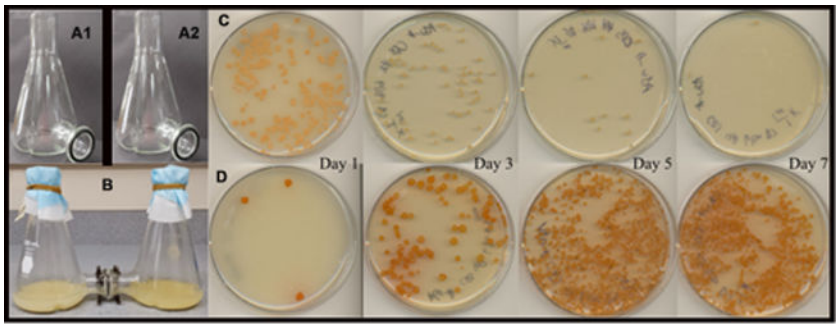

Figure 3.

Cell-cell contact study between *Micromonospora* sp. WMMB-235 and *Rhodococcus* sp. WMMA-185. (**A1** and **A2**) Each half of custom co-culture vessel enabling separation of two independent cultures with 0.2 μm filter. (**B**) Intact co-culture vessel with filter membrane separating cell types. (**C**) Aliquots of the *Rhodococcus* sp. and (**D**) aliquots of the *Micromonospora* sp. removed from culture, diluted, and streaked every 2 d.

Author Manuscript Author Manuscript Author Manuscript Author Manuscript

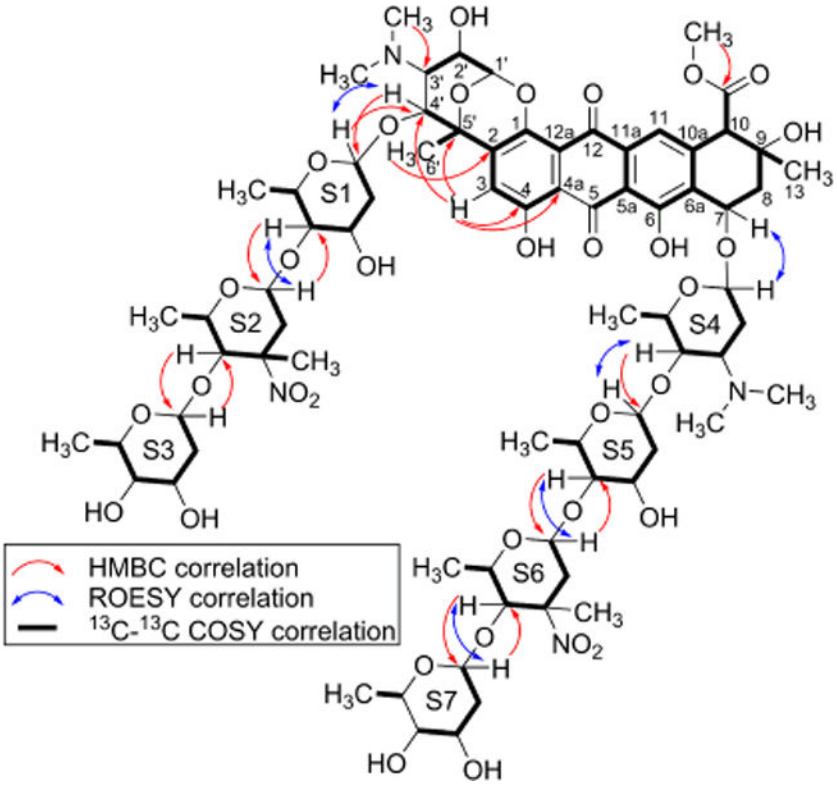

Figure 4.

Key HMBC (red) and ROESY (blue) correlations in core of (**1**) and for determination of glycosidic linkages. Carbon connectivities determined by ^{13}C–^{13}C COSY correlations (red). Detailed application of specific ROESY correlations were instrumental in determining S1–S7 configurations (Supporting Information).

Author Manuscript Author Manuscript Author Manuscript Author Manuscript

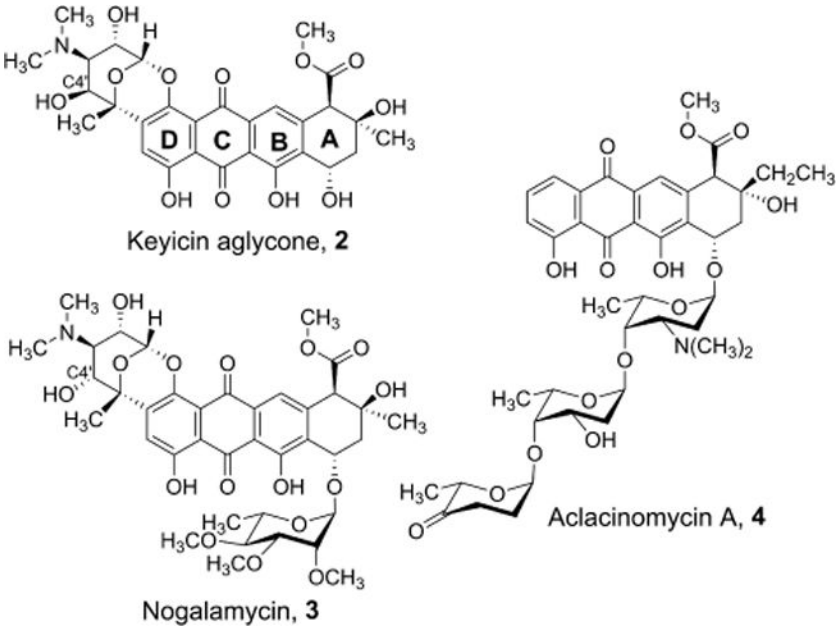

Figure 5.

Direct comparisons of the keyicin aglycone core to the intact structure of nogalamycin and the more classically arranged anthracycline aclacinomycin A.

Author Manuscript Author Manuscript Author Manuscript Author Manuscript

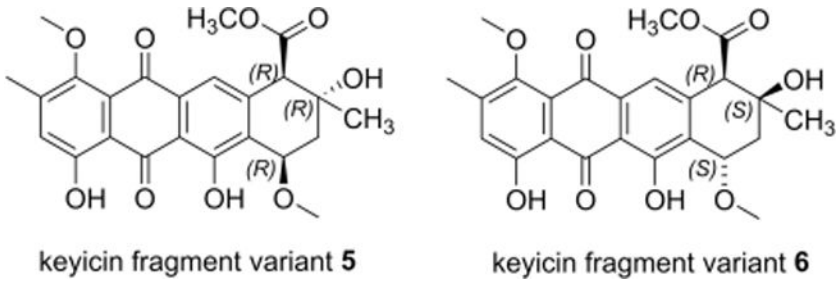

Figure 6.

Partial characterization of anthracycline core possibilities for keyicin *via* application of molecular modeling and DFT calculation approaches. See Supporting Information for experimental data for these and alternative variants.

Author Manuscript Author Manuscript Author Manuscript Author Manuscript

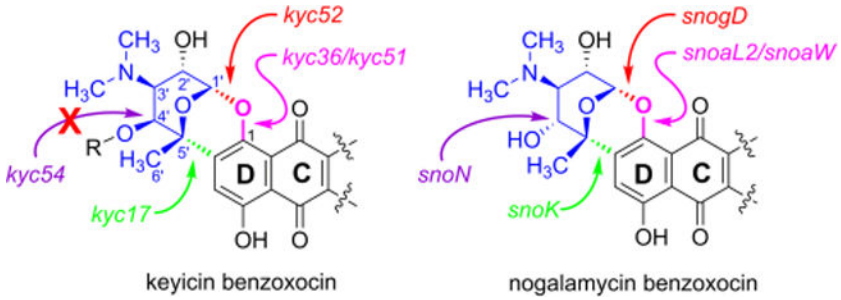

Figure 7.

Correlations of *orfs* (and resulting gene products) to key benzoxocin linkages for keyicin versus nogalamycin aglycones. Gene/enzyme similarities across the two NP systems are color coded with arrows indicating key linkages installed. Notably only *kyc54* and *snoN* appear to be similar yet fail to carry out the same chemistry upon their respective substrates.

Author Manuscript Author Manuscript Author Manuscript Author Manuscript

Table 1

Selection of key BGC gene correlations between keyicin and nogalamycin clusters

kyc gene	Nogalamycin BGC gene	Accession # for *kyc* gene	Accession # for nogalamycin gene	Putative function for established gene product	% identity
kyc9	*snoaM*[51]	OHX01513.1	AAF01818.1	polyketide cyclase	78%
kyc17	*snoK*[44]	OHX01520.1	AAF01812.1	non-heme iron α-ketoglutarate (α-KG)–dependent carbocyclase	62%
kyc25	*snogE*[51-53]	OHX01526.1	AAF01809.1	GT for nogalose	62%
kyc34	*snoaL*[48]	OHX01535.1	AAF01813.1	nogalonic acid methyl ester (NAME) cyclase	77.8%
kyc36	*snoaW*[49, 54]	OHX01536.1	AAF01810.1	putative hydroxylase (in tandem with SnoaL2)	60.7%
kyc44	*snogA*[55]	OHX01543.1	AAF01819.1	amino methyltransferase	67.2%
kyc51	*snoaL2*[49]	OHX01549.1	AAF01808.1	C-1 hydroxylase component (in tandem with SnogW)	63.2%
kyc52	*snogD*[50, 52, 53]	OHX01550.1	AAF01811.1	GT (specifically, nogalamine-transferase)	65%
kyc54	*snoN*[44]	OHX01552.1	AAF01805.1	SnoK homolog with epimerase role	71%

ACS Chem Biol. Author manuscript; available in PMC 2018 December 15.